International Journal of Pure and Applied Mathematics
Volume 74 No. 3 2012, 339-352
ISSN: 1311-8080 (printed version)
url: http://www.ijpam.eu

ijpam.eu

STRESS AND STRAIN ANALYSIS OF ROTATING FGM THERMOELASTIC CIRCULAR DISK BY USING FEM

J.N. Sharma[1], Dinkar Sharma[2 §], Sheo Kumar[3]

[1]Department of Mathematics
National Institute of Technology
Hamirpur, 177005, INDIA

[2,3]Department of Mathematics
Dr. B.R. Ambedkar National Institute of Technology
Jalandhar, 144011, INDIA

Abstract: This paper concentrates on the finite element analysis of thermoelastic stresses, displacements and strains in a thin circular functionally graded material (FGM) disk subjected to thermal loads. Further the temperature profiles have been modeled with the help of heat conduction equation. The model has been solved numerically for an Al2O3/Al FGM disk. The numerical results reveal that these quantities are significantly influenced by temperature distribution.

AMS Subject Classification: 80Axx
Key Words: FGM, circular disk, thermal field, FEM, stress, strain

1. Introduction

The finite element method is well addressed and needs less computation in addition to high accuracy in literature, Reddy [1] and Hutton [2]. Some researchers [3-8] have performed the finite element analysis of circular plates, bladed disc, circular disk, circular and annular plates, annular disks. Yong-

Received: September 3, 2011

§Correspondence author

dong et al. [9] and Zhong and Yu [10] carried out the stress analysis of FGM beams of rectangular cross section due to mechanical loads. Mote [11] used the Rayleigh-Ritz technique to investigate the free vibration characteristics of centrally clamped, variable thickness axisymmetric disks with axisymmetric in-plane stress distributions. Mote [12] studied the vibrations of non-axisymmetric disks using the finite element technique. Nigh and Olson [13] employed finite element method for rotating disks in body-fixed or a space-fixed co-ordinate system. Stress distribution in rotating composite structures of FGM solid disks have been studied by Zenkour [14]. An analysis of the thermal stress behavior of FGM hollow circular cylinders have been carried out by Liew et al. [15]. Finite element analysis of thermoelastic contact problem in functionally graded axisymmetric brake disks has been performed by Shahzamanian et al. [16]. Afsar and Go [17] studied thermoelastic field in a rotating FGM circular disk with the help of finite element method by considering uniform exponential and parabolic profiles of temperature variations. In the present paper finite element technique is used to evaluate the components of stress, strain and displacement in a rotating FGM circular disk. The thermal variations have been modeled from the heat conduction equation in case of uniform and steady state temperature distributions. The case of FGM non-heat conducting circular disk has also been considered in which the prevailing conditions are isentropic and the thermal field is expressed by a temperature relation in terms of strains in the disk. The results have been found in close agreement with those available in literature and consistent with physical situations.

2. Mathematical Model

We consider a circular disk with a concentric circular hole as shown in Fig. 1. The disk is assumed to be rotating with angular frequency ω. The origin of the polar co-ordinate system $r-\theta$ is assumed to be located at the center of the disk and hole. The disk is considered to be composed of two distinct material phases A and B whose distribution varies continuously along the radial direction only. This makes the problem axisymmetric and hence the field quantities are independent of θ so that $\frac{\partial}{\partial\theta}=0$.

Because the material distribution and properties of the FGM disk are functions of r only, therefore it is assumed that the Young's modulus E, coefficient of thermal expansion α and density ρ of the disk vary exponentially according as:

$$E=E_0e^{\beta r},\quad \alpha=\alpha_0e^{\gamma r},\quad \rho=\rho_0e^{\mu r}. \tag{1}$$

As the inner surface of the FGM disk consists of material A and outer surface of material B, therefore the constants in equation (1) are determined as [17]

$$E_0 = E_A e^{\beta r}, \quad \alpha_0 = \alpha_A e^{\gamma r}, \quad \rho_0 = \rho_A e^{\mu r}, \tag{2}$$

$$\beta = \frac{1}{a-b} ln(E_A/E_B), \quad \gamma = \frac{1}{a-b} ln(\alpha_A/\alpha_B), \quad \mu = \frac{1}{a-b} ln(\mu_A/\mu_B). \tag{3}$$

Here, the subscripts A and B of a variable are used to denote the properties of the constituent materials A and B, respectively. The disk has a small constant thickness and hence the instant analysis is carried out under plane stress conditions.

3. Boundary Conditions

The FGM disk considered in the present study is subjected to a temperature gradient field. The inner surface of the disk is assumed to be fixed to a shaft so that isothermal conditions prevail on it. The outer surface of the disk is free from any mechanical load and maintained at uniform temperature gradient. Thus, the boundary conditions of the problem are given by:

$$\begin{aligned} &(i) \qquad r = a, \quad u_r = 0, \quad T = 0, \\ &(ii) \qquad r = b, \quad \sigma_r = 0, \quad \frac{dT}{dr} = T_0, \end{aligned} \tag{4}$$

where u_r and σ_r denote displacement and stress along the radial direction.

4. Formulation of the Problem

The materials of the disk experience a stress due to incompatible eigenstrain when subjected to a temperature gradient field. The disk being isotropic leads to a thermal eigenstrain at a point which remains same in all directions and is given by

$$\varepsilon^* = \alpha(r) T(r), \tag{5}$$

where $T(r)$ is the change in temperatures at any distance r. Thus the components of the total strain are given by

$$\varepsilon_r = e_r + \varepsilon^*, \quad \varepsilon_\theta = e_\theta + \varepsilon^*, \tag{6}$$

where ε_r and ε_θ are the radial and circumferential components of the total strain and e_r and e_θ are the radial and circumferential components of the elastic strain. Due to symmetry considerations, the shear strains do not play any role. The Hooke's law provides us

$$\varepsilon_r = \frac{1}{E}(\sigma_r - \nu\sigma_\theta) + \varepsilon^*, \quad \varepsilon_\theta = \frac{1}{E}(\sigma_\theta - \nu\sigma_r) + \varepsilon^* \tag{7}$$

where σ_r and σ_θ are the radial and circumferential stress components, respectively. Here ν is the Poisson ratio of the material. The two-dimensional equilibrium equations in polar co-ordinate for a rotating disk are given by

$$\frac{\partial\sigma_r}{\partial r} + \frac{1}{r}\frac{\partial\tau_{r\theta}}{\partial\theta} + \frac{\sigma_r - \sigma_\theta}{r} + \rho\omega^2 r = 0, \tag{8}$$

$$\frac{\partial\tau_{r\theta}}{\partial r} + \frac{1}{r}\frac{\partial\sigma_\theta}{\partial\theta} + \frac{2\tau_{r\theta}}{r} = 0, \tag{9}$$

where last term in the first equation corresponds to the inertia force due to rotation of the disk. Because of symmetry, the second equilibrium equation of system of equation (8) is identically satisfied and the first equilibrium reduces to

$$\frac{d}{dr}(r\sigma_r) - \sigma_\theta + \rho\omega^2 r^2 = 0. \tag{10}$$

Upon substituting $F = r\sigma_r$ in equations (10) and (7), we get

$$\sigma_\theta = \frac{dF}{dr} + \rho\omega^2 r^2 \tag{11}$$

$$\varepsilon_r = \frac{1}{E}\left(\frac{F}{r} - \nu\frac{dF}{dr}\right) - \frac{\nu\rho}{E}\omega^2 r^2 + \varepsilon^* \tag{12}$$

$$\varepsilon_\theta = \frac{1}{E}\left(\frac{dF}{dr} - \frac{\nu F}{r}\right) + \frac{\rho}{E}\omega^2 r^2 + \varepsilon^*. \tag{13}$$

The two strain components are related by

$$\varepsilon_r = \frac{d}{dr}(r\varepsilon_\theta).$$

Using equation (11) in equation (12), we obtain

$$\frac{d^2F}{dr^2} + \left(\frac{1}{r} - \beta\right)\frac{dF}{dr} + \frac{1}{r}\left(\beta\nu - \frac{1}{r}\right)F$$

$$= \rho\omega^2 r\left(\beta r - \mu r - \nu - 3\right) - E\alpha\left(\gamma T + \frac{dT}{dr}\right). \quad (14)$$

The heat conduction equation for a dynamic coupled thermoelastic solid is given by [Dhaliwal and Singh [18]]

$$K\left(\frac{\partial^2}{\partial r^2} + \frac{1}{r}\frac{\partial}{\partial r}\right)T - \rho C_e\frac{\partial T}{\partial t} = \frac{E\alpha T_0(\dot{e_r} + \dot{e_\theta})}{1-\nu}, \quad (15)$$

where K is the thermal conductivity, C_e -Specific heat at constant strain and T_0 being uniform reference temperature. The equations (13) and (14) are the governing second order differential equation which provides us the function F and hence the components of stress.

5. Temperature Field

We shall consider following three cases of thermal variations in the FGM disk: Case I: Disk having uniform temperature distribution. In this case, we have

$$T(r) = T_0, \quad \frac{dT}{dr} = 0. \quad (16)$$

Case II: Disk at steady state temperature distribution. In this case $\frac{\partial}{\partial t} \cong 0$, so that the heat conduction equation (14) takes the form

$$\left(\frac{d^2}{dr^2} + \frac{1}{r}\frac{d}{dr}\right)T = 0.$$

Upon solving this equation with the help of thermal conditions (4), we obtain

$$T(r) = bT_0\log(r/a), \quad \frac{dT}{dr} = \frac{bT_0}{r}. \quad (17)$$

Case III: Non-heat conducting (isentropic) disk. In this case thermal conductivity $K = 0$ so that equation (14) leads to the temperature relation given by

$$T = \frac{-T_0 E\alpha}{\rho C_e(1-\nu)}\left(e_r + e_\theta\right). \quad (18)$$

Here the prevailing thermo-dynamical conditions in the FGM circular disk are of constant entropy (isentropic) and it is assumed that initially the disk is

at uniform temperature T_0. Upon substituting the values of e_r and e_θ from equations (11) into equation (17) and rearranging the terms, we get

$$T(r) = \frac{-T_0\alpha}{\rho C_e}\left(\frac{dF}{dr} + \frac{1}{r}F + \rho\omega^2 r^2\right), \tag{19}$$

$$\frac{dT}{dr} = A\left(-\frac{d^2F}{dr^2} + B\frac{dF}{dr} + C\frac{F}{r} + D\rho\omega^2 r^2\right), \tag{20}$$

where

$$\begin{aligned} 2A &= \frac{T_0\alpha}{\rho C_e}, & B &= \frac{(\mu r - \gamma r - 1)}{r}, \\ C &= \frac{(\mu r - \gamma r + 1)}{r}, & D &= -(2 + \gamma r). \end{aligned} \tag{21}$$

These temperature distributions given by equations (15), (16) and (18) holds in the domain $a \le r \le b$.

6. Finite Element Formulation

Substituting the values of T and $\frac{dT}{dr}$ from equations (16) and (18)-(20) in equation (13) and following a standard finite element discretization approach, the domain of the disk is divided radially into N number of elements of equal size and consequently the equation (13) can be transformed to the following system of simultaneous algebraic equations for Cases I, II and III:

$$\sum_{j=1}^{2} K_{ij}^e F_j^e = L_i^e; \quad i = 1, 2,\ e = 1, 2, ..., N. \tag{22}$$

The quantities K_{ij}^e and F_j^e in respective cases are given by: Case I and II:

$$K_{ij}^e = \int_{r_e}^{r_{e+1}} \frac{d\phi_i^e}{dr}\frac{d\phi_j^e}{dr}dr - \int_{r_e}^{r_{e+1}} \left(\frac{1}{r} - \beta\right)\phi_i^e \frac{d\phi_j^e}{dr}dr - \int_{r_e}^{r_{e+1}} \frac{1}{r}\left(\beta\nu - \frac{1}{r}\right)\phi_i^e\phi_j^e dr,$$

$$L_i^e = \int_{r_e}^{r_{e+1}} \phi_i^e f(r)dr + \phi_i^e(r_{e+1})\frac{d\phi_j^e}{dr}(r_{e+1}) - \phi_i^e(r_e)\frac{d\phi_j^e}{dr}(r_e).$$

Case I:

$$P = \frac{1}{r} - \beta, \quad Q = \left(\beta\nu - \frac{1}{r}\right),$$

$$R = \mu r + \nu + 3 - \beta r, \quad S = -E\alpha\gamma T_0.$$

Case II:

$$P = \frac{1}{r} - \beta, \quad Q = \left(\beta\nu - \frac{1}{r}\right),$$

$$R = \mu r + \nu + 3 - \beta r, \quad S = -bE\alpha T_0 \left(\frac{1}{r} + \gamma \log \frac{r}{a}\right). \tag{23}$$

Case III:

$$P = \left(\frac{C_e\rho(1 - r\beta) + ET_0\alpha^2(\mu r - 2\gamma r - 1)}{r(C_e\rho - E\alpha^2)T_0}\right),$$

$$Q = \left(\frac{C_e\rho(\beta\nu r - 1) + ET_0\alpha^2(\mu r - 2\gamma r - 1)}{r(C_e\rho - E\alpha^2)T_0}\right),$$

$$R = -[E\alpha(2 + 2\gamma r) + (\beta r - \mu r - \nu - 3)],$$

$$S = 0, \tag{24}$$

$$f(r) = E\alpha\gamma T_0 - \rho\omega^2 r(\beta r - \mu r - \nu - 3), \quad \text{for Case I.}$$

$$f(r) = E\alpha(\gamma bT_0 \log \frac{r}{a} + \frac{bT_0}{r}) - \rho\omega^2 r(\beta r - \mu r - \nu - 3), \quad \text{for Case II.} \tag{25}$$

$$\phi_1^e = \frac{r_{e+1} - r}{r_{e+1} - r_e}, \quad \phi_2^e = \frac{r - r_e}{r_{e+1} - r_e}. \tag{26}$$

Here the superscript e indicates the element number used to discretize the domain of the disk.

Case III: In this case the quantities K_{ij}^e and L_i^e are given by

$$K_{ij}^e = \int_{r_e}^{r_{e+1}} \frac{d\phi_i^e}{dr}\frac{d\phi_j^e}{dr}dr - \int_{r_e}^{r_{e+1}} P\phi_i^e\frac{d\phi_j^e}{dr}dr - \int_{r_e}^{r_{e+1}} Q\frac{1}{r}\phi_i^e\phi_j^e dr, \tag{27}$$

$$L_i^e = \int_{r_e}^{r_{e+1}} \phi_i^e f(r)dr + \phi_i^e(r_{e+1})\frac{d\phi_j^e}{dr}(r_{e+1}) - \phi_i^e(r_e)\frac{d\phi_j^e}{dr}(r_e), \tag{28}$$

where $f(r) = R\rho\omega^2 r$ and ϕ_1^e,ϕ_2^e are defined in equation (27). The solution in each case gives the values of F_j^e at different nodal points of the disk, which further used to calculate the components of stress, strain and displacement from the relations given below:

$$\sigma_r = \frac{1}{r}\sum_{j=1}^{2} F_j^e\phi_j^e, \sigma_\theta = \sum_{j=1}^{2} F_j^e\frac{d\phi_j^e}{dr} + \rho\omega^2 r^2,$$

$$\varepsilon_r = \frac{1}{E}\sum_{j=1}^{2}\left[\frac{F_j^e\phi_j^e}{r} - \nu F_j^e\frac{d\phi_j^e}{dr}\right] - \frac{\nu\rho\omega^2 r^2}{E} + \varepsilon^*,$$

$$\varepsilon_\theta = \frac{1}{E}\sum_{j=1}^{2}\left[F_j^e\frac{d\phi_j^e}{dr} - \frac{\nu}{r}F_j^e\phi_j^e\right] + \frac{\nu\rho\omega^2 r^2}{E} + \varepsilon^*,$$

$$u_r = \frac{r}{E}\sum_{j=1}^{2}\left[F_j^e\frac{d\phi_j^e}{dr} - \frac{\nu}{r}F_j^e\phi_j^e\right] + \frac{\nu\rho\omega^2 r^3}{E} + r\varepsilon^*. \tag{29}$$

This completes the finite element formulation of the problem. For uniform temperature distribution (Case I) the analysis agrees with Afsar and Go [17].

7. Numerical Results and Discussion

In this section, some numerical results of different components of stress, strain and displacement have been computed for an Al_2O_3/Al FGM disk in which the ingredient materials Al and Al_2O_3 correspond to the materials A and B, respectively. The mechanical and thermal properties of these ingredient materials are that of Afsar [17].

The value of Poisson's ratio has been taken $\nu = 0.3$ which remains constant throughout the material. Here we have taken $a = 15mm$ and $b = 150mm$. The element size is chosen as $1mm$ in numerical calculations of all the results presented in this section. The angular speed $\omega = 1rad/s$ and the ratio of the outer radius to the inner radius $b/a = 10$. Variations of different components of stress, strain and displacement for Case I, Case II and non-conducting coupled disk (Case III) versus $(r-a)/(b-a)$ have been presented in Figures 2-6. Figure 2 shows the variations of radial stress distribution for Case I, Case II and Case III temperature distributions versus $(r-a)/(b-a)$. It is noticed that the radial stress initially decreases to attain its minimum value in each case which then increases in a steady manner in Case II and III in contrast to that in Case I where it is subjected to a sharp increase for $(r-a)/(b-a) \geq 0.8$ to become zero at the boundary. The magnitude of radial stress component attains lowest value for uniform temperature variation (Case I) as compared to that of Case II and III. Thus, if the inner surface of the disk is maintained at low temperature by cooling processes during cutting or grinding, the radial stress can be controlled to the minimum. Figure 3 reveals that the circumferential stress in a circular FGM disk for uniform temperature (Case I) and Cases II and III of variable temperatures increases initially before it becomes

steady and finally observes increasing trend to attain its maximum value at the boundary. The profiles of this quantity are noticed to be fashioned in a similar manner in each case except some crossover points in Cases II and III and difference in its magnitude. Figures 4 and 5 illustrate the distribution of radial and circumferential strains, respectively. It is observed that the radial strain component is maximum at the inner surface of the disk and its magnitude gradually decreases towards the outer surface of the disk. The uniform temperature (Case I) yields the minimum radial strain as compared to that in Case II and Case III. The circumferential strain component attains the maximum value for non-conducting disk (Case III) and minimum for the uniform temperature distribution (Case I). However, the circumferential strain is zero at the inner surface of the disk in each case. Figure 6 presents the variations of displacement in Case I to III of temperature variation. It obviously satisfies the initial and boundary conditions. The displacement gradually increases from its zero value at the inner surface to the maximum value at the outer surface of the disk in all the considered cases of thermal variations. The comparison of the profiles of various considered quantities exhibit more or less the similar type of behavior and trend of variations as that of Afsar and Go [17] though these get smoothened and refined in the present cases.

8. Conclusions

It is concluded that the stress, strain and displacement of FGM circular disk for fixed angular velocity get significantly modified due to uniform temperature variation, logarithmic thermal changes and non-heat conducting (isentropic) conditions. The circumferential stress is observed to be compressive in the inner region of the disk and tensile over the outer region. Significant changes have been noticed in the profiles of radial and circumferential stresses, strain and displacement with increasing ratio of difference between radial component and inner radius of disk to difference between outer and inner radii of disk. It is concluded that the thermoelastic field in an FGM disk can be modeled and optimized by controlling thermal variations, radial thickness and temperature difference at inner and outer surfaces of the disk. This study may be useful in designing with an FGM circular cutter or grinding disk for proper and reliable thermoelastic characteristics in service.

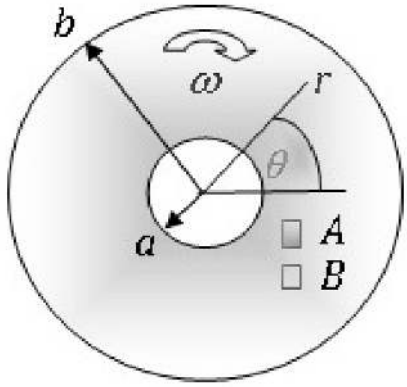

Figure 1: Geometry of Problem

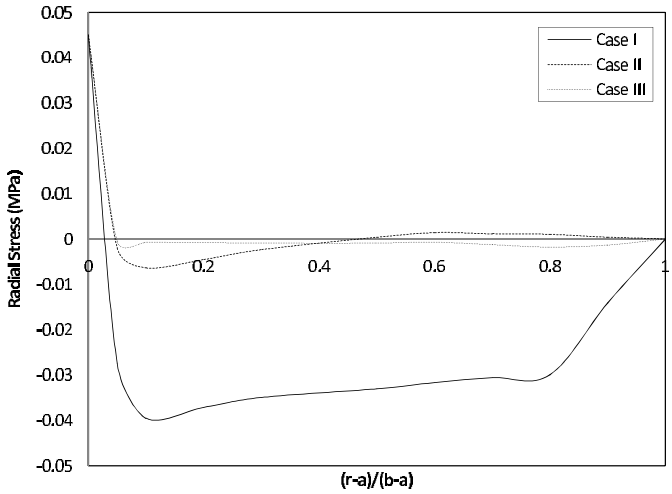

Figure 2: Radial Stress versus $(r-a)/(b-a)$ for various cases of temperature distribution.

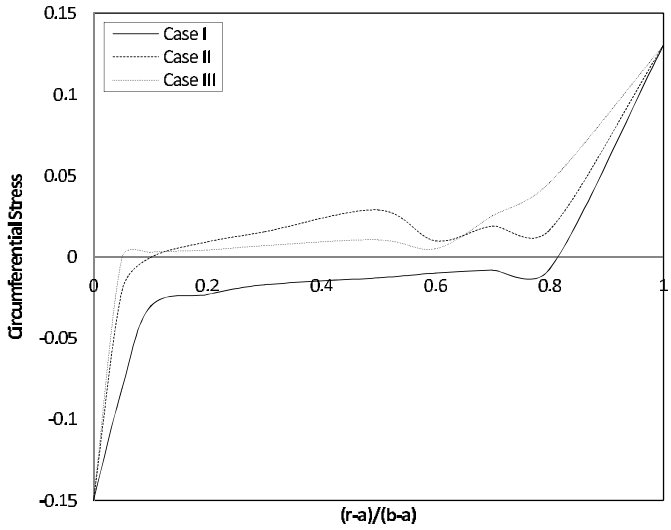

Figure 3: Circumferential Stress versus $(r-a)/(b-a)$ for various cases of temperature distribution.

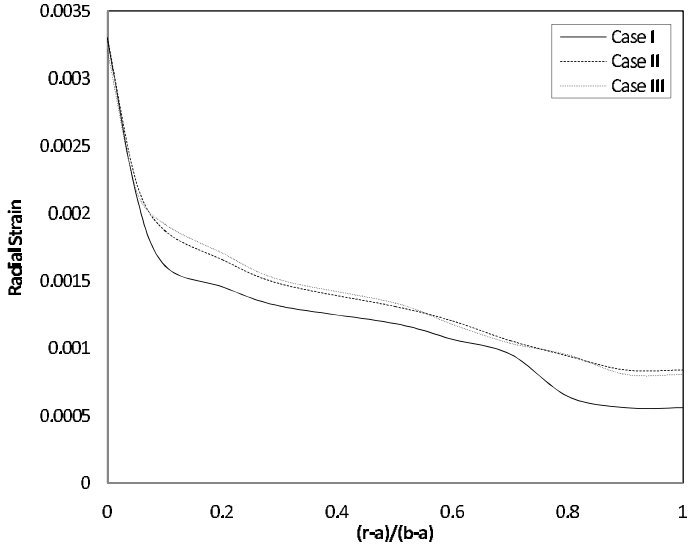

Figure 4: Radial Strain versus $(r-a)/(b-a)$ for various cases of temperature distribution.

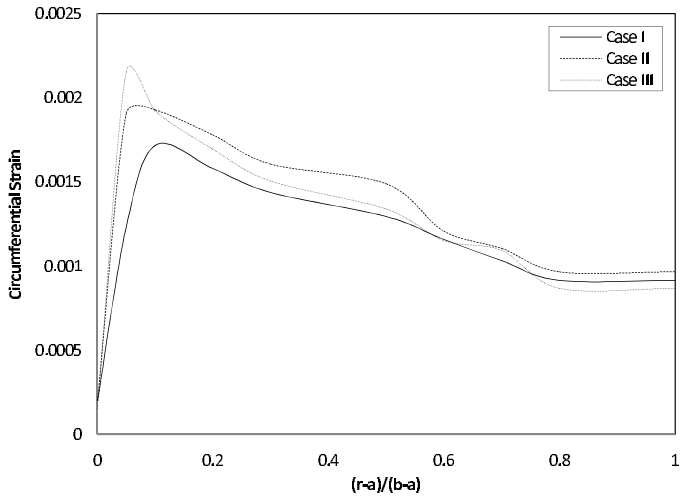

Figure 5: Circumferential Strain versus $(r-a)/(b-a)$ for various cases of temperature distribution.

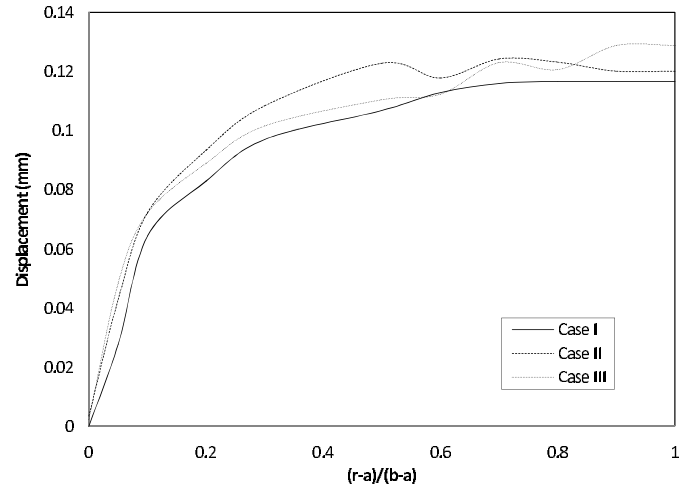

Figure 6: Displacement versus $(r-a)/(b-a)$ for various cases of temperature distribution.

References

[1] J.N. Reddy, *An Introduction to the Finite Element Method*, Tata McGraw-Hill, 3-rd Edition (2005).

[2] D.V. Hutton, *Fundamental of Finite Element Analysis*, Tata McGraw-Hill (2004).

[3] G.H. Thiel, R.E. Miller, A finite element for the linear analysis of laminated circular plates, *Comp. Struct.*, **27** (1994), 339-335.

[4] J. Kirkhope, G.J. Wilson, A finite element analysis for the vibration modes of a bladed disc, *J. Sou. Vib.*, **49** (1976), 469-482.

[5] T.K. Paul, Stresses in a thin centrally cracked circular disk, *Engng. Fra. Mech.*, **52** (1995), 139-153.

[6] C.F. Liu, G.T. Chen, A simple finite element analysis of axisymmetric vibration of annular and circular plates, *Int. J. Mech. Sci.*, **37** (1995), 861-871.

[7] V. Srinivasan, V. Ramamurti, Finite element analysis of the in-plane behavior of annular disks, *Comp. & Struct.*, 13 (1981), 553-561.

[8] H.V. Lakshminarayana, Finite element analysis of rotating laminated composite annular discs, *Composites*, **17** (1986), 42-48.

[9] L. Yongdong, Z. Hongcai, Z. Nan, D. Yao, Stress analysis of functionally gradient beam using effective principal axes, *Int. J. Mech. Mater.*, **2** (2005), 157-164.

[10] Z. Zhong, T. Yu, Analytical solution of a cantilever functionally graded beam, *Comp. Sci. Tech.*, **67** (2007), 481-488.

[11] C.D. Mote Jr., Free vibration of initially stressed circular disks, *J. Engng. Indu.*, **87** (1965), 258-264.

[12] C.D. Mote Jr., Stability control analysis of rotating plates by finite element: Emphasis on slots and holes, *J. Dynamic Sys. Measu. Cont.*, **94** (1972), 64-70.

[13] G.L. Nigh, M.D. Olson, Finite element analysis of rotating disks, *J. Sound Vib.*, **77** (1981), 61-78.

[14] A.M. Zenkour, Stress distribution in rotating composite structures of functionally graded solid disks, *J. Mater. Process. Technol.*, **209** (2009), 3511-3517.

[15] K.M. Liew, S. Kitipornchai, X.Z. Zhang, C.W. Lim, Analysis of the thermal stress behavior of functionally graded hollow circular cylinders, *Int. J. Solids Struct.*, **40** (2003), 2355-2380.

[16] M.M. Shahzamanian, B.B. Sahari, M. Bayat, F. Mustapha, Z.N. Ismarrubie, Finite element analysis of thermoelastic contact problem in functionally graded axisymmetric brake disks, *Comp. Struct.*, **92** (2010), 1591-1602.

[17] A.M. Afsar, J. Go, Finite element analysis of thermoelastic field in a rotating FGM circular disk, *Appl. Math. Mod.*, **34** (2010), 3309-3320.

[18] R.S. Dhaliwal, A. Singh, *Dynamic Coupled Thermoelasticity*, Hindustan Publishing Corporation, New Delhi, India (1980).